Int. J. Heat Mass Transfer. Vol. 32, No. 3, pp. 529–539, 1989
Printed in Great Britain

0017–9310/89 $3.00 + 0.00

Non-Darcian effects on vortex instability of a horizontal natural convection flow in a porous medium

WEN-JENG CHANG and JIIN-YUH JANG†
Department of Mechanical Engineering, National Cheng-Kung University, Tainan, Taiwan 70101, Republic of China

(*Received* 28 *April* 1988 *and in final form* 8 *August* 1988)

Abstract—The non-Darcian effects, which include the inertia, boundary and convective effects, on the flow and vortex instability of a horizontal natural convection boundary flow in a high-porosity medium are examined. In the base flow, the governing conservation equations are solved by using a suitable variable transformation and employing an implicit finite-difference scheme developed by Keller. The stability analysis is based on the linear stability theory, and the resulting equations are solved on the basis of the local similarity approximations. The results indicate that all of these three effects reduce the heat transfer rate. In addition, the combined boundary and convective effects stabilize the flow to the vortex mode of disturbance, while the inertia effect destabilizes it.

1. INTRODUCTION

THE PROBLEM of the vortex mode of instability in natural convection flow over a horizontal or an inclined heated plate in a saturated porous medium has recently received considerable attention [1–5]. This instability mechanism is due to the presence of a buoyancy force component in the direction normal to the plate surface. Hsu *et al.* [1], and Hsu and Cheng [2] analysed the vortex mode of instability of horizontal and inclined natural convection flows in porous media. Reference [3] re-examined the same problem for an inclined plate, where both the streamwise and normal components of the buoyancy force are retained in the momentum equations. Therefore, ref. [3] provides new vortex instability results for small angles of inclination from the horizontal ($\phi \leqslant 30°$) and more accurate results for large angles of inclination ($\phi > 30°$) than the previous study [2]. Reference [4] studied the vortex instability of horizontal natural convection in porous media resulting from combined heat and mass buoyancy effects. Reference [5] also examined the effects of density extremum on the vortex instability of an inclined buoyant layer in porous media saturated with cold water. All of these works are based on the Darcy formulation. However, at a higher Rayleigh number or in a high porosity medium, there is a departure from Darcy's law and the inertia (velocity-squared term), boundary (no-slip condition) and convective (development term) effects not included in the Darcy model may become significant.

The earliest non-Darcy flow model for the inertia effect is that proposed by Forchheimer [6]. Plumb and Huenefeld [7] studied the inertia effect in free convection from a vertical plate embedded in a porous medium based on Forchheimer's model. Bejan and Poulikakos [8] reconsidered the problem and presented boundary layer solutions for the intermediate and non-Darcy flow regimes to supplement the boundary-layer analysis of Cheng and Minkowycz [9] for Darcy's law. Their results indicate that the heat transfer rate decreases when the flow regime changes from Darcy to non-Darcy.

Brinkman [10] and Chan *et al.* [11] argued that the momentum equation for porous media flow must reduce to the viscous flow limit and advocated that classical frictional terms be added in Darcy's law as the permeability is high. This is known as the Brinkman model. The Brinkman model was used by Hsu and Cheng [12] to study the natural convection about a semi-infinite vertical flat plate in a porous medium, by Tong and Subramanian [13] and by Vasseur and Robilland [14] to study the natural convection in a vertical porous enclosure. It was also used by Katto and Masuaka [15] as well as by Walker and Homsy [16] for the studies of onset of free convection of liquids in a porous medium bounded between parallel plates and heated from below.

Vafai and Tien [17] investigated the inertia and boundary effects in forced convection over a horizontal plate based on the volume averaging technique. An error map on the basis of numerical results has been presented to illustrate the domain of applicability of Darcy's law. Evans and Plumb [18] have examined the problem of natural convection about a vertical plate numerically based on Brinkman's model with the addition of convective terms. The significance of the boundary, convective and inertia effects on natural convection from a vertical flat plate embedded in a

† Author to whom correspondence should be addressed.

NOMENCLATURE

a dimensional spanwise wave number
C inertia coefficient
Da_x Darcy number, K/x^2
f dimensionless stream function
F dimensionless disturbance stream function amplitude
Fr Forchheimer number, $5g\beta AK^{5/2}c^2/\nu^2$
g gravitational acceleration
G $Gr_x/5$
Gr local Grashof number, $g\beta\Delta Tx^3/\nu^2$
k dimensionless wave number, $ax/G^{1/5}$
K permeability
m exponent on wall temperature relation
Nu_x local Nusselt number
p motion pressure
p' perturbation pressure
Pr Prandtl number
Q dimensionless disturbance velocity in the x-direction
T temperature
T' perturbation temperature
$\tilde{T}$ disturbance temperature amplitude
$\tilde{u}$ x-direction disturbance velocity amplitude
u, v, w volume averaged velocity in the x-, y-, z-directions
u', v', w' disturbance velocity in the x-, y-, z-directions
x, y, z axial, normal and spanwise coordinates.

Greek symbols
α effective thermal diffusivity
β coefficient of thermal expansion
ε porosity
ξ parameter, $1/D_x G^{2/5}$
η pseudo similarity variable
θ dimensionless temperature, $(T-T_\infty)/(T_w-T_\infty)$
Θ dimensionless disturbance temperature amplitude
μ, ν absolute and kinematic viscosity
ρ density
ψ stream function
ψ' disturbance stream function
$\tilde{\psi}$ disturbance stream function amplitude.

Subscripts
w condition at the wall
∞ condition at the free stream.

Superscript
* critical condition.

high-porosity medium is investigated by Hong *et al.* [19]. However, the non-Darcian behaviour on the vortex mode of instability in a porous medium seems not to have been investigated. This motivated the present investigation.

The purpose of this paper is to examine the inertia, boundary and convective effects on the vortex instability of a horizontal natural convection flow in a high-porosity medium. In the main flow, the boundary layer approximations are invoked, and the resulting governing equations are solved by using a suitable variable transformation and employing an efficient finite-difference method similar to that described in Cebeci and Bradshaw [20]. The stability analysis is based on the linear stability theory. The disturbance quantities are assumed to be of the form of a stationary vortex roll that is periodic in the spanwise direction, with its amplitude function depending primarily on the normal coordinate and weakly on the streamwise coordinate [2]. The resulting eigenvalue problem is solved by using a variable step-size sixth-order Runge–Kutta integration scheme incorporated with the Gram–Schmidt orthogonalization procedure [21] to maintain the linear independence of the eigenfunctions.

2. MATHEMATICAL FORMULATION

The physical model considered in this paper consists of a semi-infinite, horizontal plate, with a power law variation of wall temperature, i.e. $T_w = T_\infty + Ax^m$ (where A and m are constants), embedded in a porous medium (T_∞). The x and z coordinates are placed on the horizontal surface and the y coordinate is perpendicular to the surface and points toward the porous medium. In order to study transport through high-porosity media, the original Darcy model is improved by including inertia, boundary and convective effects using volume-averaged principles and empirical results [17]. In addition, if we assume that: (1) properties of the fluid except for the density term that is associated with the body force are constant, (2) the porous medium is everywhere isotropic and homogeneous, and (3) the Boussinesq approximation is employed, then the conservation equations become

$$\nabla \cdot u = 0 \tag{1}$$

$$\frac{\rho}{\varepsilon^2} u \cdot \nabla u = -\nabla p + \rho g \beta (T - T_\infty) j - \frac{\mu}{K} u - \rho c |u| u + \frac{\mu}{\varepsilon} \nabla^2 u \tag{2}$$

$$u \cdot \nabla T = \alpha \nabla^2 T \tag{3}$$

where K and C are the permeability and the inertia coefficient of the porous medium; j the unit vector opposite to gravity; α the effective thermal diffusivity

of the medium, and p the motion pressure. The other various symbols are defined in the Nomenclature.

Before proceeding to the instability problem, consideration is given first to the basic natural convection flow along a horizontal surface, since the computation of instability criteria requires a knowledge of the velocity and temperature profiles for the main flow and the solution has not been investigated before.

2.1. *The main flow and thermal fields*

By applying the boundary layer assumptions for the two-dimensional flow, the governing equations, equations (1)–(3), become

$$\frac{\partial u}{\partial x}+\frac{\partial v}{\partial y}=0 \tag{4}$$

$$\frac{\rho}{\varepsilon^2}\left(u\frac{\partial u}{\partial x}+v\frac{\partial u}{\partial y}\right)=\frac{\mu}{\varepsilon}\frac{\partial^2 u}{\partial y^2}-\frac{\mu}{K}u-\rho c u^2-\frac{\partial p}{\partial x} \tag{5}$$

$$0=\rho g\beta(T-T_\infty)-\frac{\partial p}{\partial y} \tag{6}$$

$$u\frac{\partial T}{\partial x}+v\frac{\partial T}{\partial y}=\alpha\frac{\partial^2 T}{\partial y^2}. \tag{7}$$

The streamwise pressure gradient in equation (5) induced by the buoyancy force can be related to the temperature difference through equation (6) as

$$-\frac{\partial p}{\partial x}=\rho g\beta\frac{\partial}{\partial x}\int_y^\infty (T-T_\infty)\,\mathrm{d}y. \tag{8}$$

These are subjected to the following boundary conditions:

$$\begin{aligned} &y=0, \quad u=v=0, \quad T=T_\infty+Ax^m\\ &y\to\infty, \quad u=0, \quad\quad T=T_\infty. \end{aligned} \tag{9}$$

We introduce the following transformations:

$$\eta(x,y)=\frac{y}{x}G^{1/5}, \quad \xi=\xi(x)$$

$$f=\frac{\psi}{5\nu G^{1/5}}, \quad \theta=\frac{T-T_\infty}{T_w-T_\infty}=\frac{T-T_\infty}{\Delta T} \tag{10}$$

where $G=Gr_x/5$ and $Gr_x=g\beta\Delta T x^3/\nu^2$ is the local Grashof number. ψ is the stream function which automatically satisfies continuity equation (4). The coordinate $\xi(x)$ is so chosen that x does not appear explicitly in either the transformed equations or the transformed boundary conditions.

Substituting equations (10) into equations (4)–(8), we obtain

$$\begin{aligned} &\frac{1}{\varepsilon}f'''+\frac{1}{\varepsilon^2}\{(m+3)ff''-(2m+1)f'^2\}-\xi f'\\ &\quad-\xi^{5/(4-2m)}Fr^{1/(2-m)}f'^2-\frac{m-2}{5}\eta\theta+\frac{4m+2}{5}\int_\eta^\infty\theta\,\mathrm{d}\eta\\ &=(4-2m)\xi\left[\frac{1}{\varepsilon^2}f'\frac{\partial f'}{\partial\xi}-\frac{1}{\varepsilon^2}f''\frac{\partial f}{\partial\xi}-\frac{1}{5}\frac{\partial}{\partial\xi}\int_\eta^\infty\theta\,\mathrm{d}\eta\right] \end{aligned} \tag{11}$$

$$\begin{aligned} &\theta''-5mPrf'\theta+(m+3)Prf\theta'\\ &\quad=(4-2m)Pr\xi\left[f'\frac{\partial\theta}{\partial\xi}-\theta'\frac{\partial f}{\partial\xi}\right] \end{aligned} \tag{12}$$

and the transformed boundary conditions are

$$\begin{aligned} &f(\xi,0)=0, \quad f'(\xi,0)=0, \quad \theta(\xi,0)=1\\ &f'(\xi,\infty)=0, \quad \theta(\xi,\infty)=0. \end{aligned} \tag{13}$$

In the foregoing equations, primes denote partial differentiation with respect to η

$$Fr=(5g\beta AK^{5/2}c^2)/\nu^2$$

is the Forchheimer number expressing the relative importance of the inertia effect, and Pr the Prandtl number. ξ is found to have the expression

$$\xi(x)=\frac{1}{Da_x G^{2/5}}\propto\frac{x^{4/5}}{K(T_w-T_\infty)^{2/5}} \tag{14}$$

where $Da_x=K/x^2$ is the local Darcy number. The parameter, ξ, characterizes the local vigour of the flow ($\Delta T=T_w-T_\infty$), the distance along the plate from the leading edge (x), and the permeability (K) of the porous medium. As x increases or ΔT, K decrease, the value of $\xi(x)$ increases. It is noted that Darcy's law corresponds to the case of $\xi\to\infty$ (i.e. $K\to 0$) with $Fr=0$.

In terms of new variables, it can be shown that the velocity components and local Nusselt number are given by

$$u=\frac{5\nu G^{2/5}}{x}f'$$

$$v=-\frac{\nu}{x}G^{1/5}\left[(m+3)f+(4-2m)\xi\frac{\partial f}{\partial\xi}+(m-2)\eta f'\right]$$

$$Nu_x=-\theta'(\xi,0)G^{1/5}. \tag{15}$$

2.2. *The disturbance flow*

In the usual manner for stability analysis, the velocity, pressure and temperature are assumed to be the sum of a mean and fluctuating component, here designated as barred and primed quantities, respectively. We assume that the derivatives of the perturbation quantities with respect to x may not be zero. Hence, the perturbed flow can be represented as

$$\begin{aligned} u(x,y,z)&=\bar{u}(x,y)+u'(x,y,z)\\ v(x,y,z)&=\bar{v}(x,y)+v'(x,y,z)\\ w(x,y,z)&=w'(x,y,z)\\ T(x,y,z)&=\bar{T}(x,y)+T'(x,y,z)\\ P(x,y,z)&=\bar{P}(x,y)+P'(x,y,z). \end{aligned} \tag{16}$$

After substituting equations (16) into the governing equations for the three-dimensional convective flow in a porous medium, subtracting the parts satisfied by the base quantities, and linearizing the disturbance

quantities, we arrive at the following equations for the disturbances :

$$\frac{\partial u'}{\partial x}+\frac{\partial v'}{\partial y}+\frac{\partial w'}{\partial z}=0 \tag{17}$$

$$\frac{\rho}{\varepsilon^2}\left[u'\frac{\partial \bar{u}}{\partial x}+\bar{u}\frac{\partial u'}{\partial x}+v'\frac{\partial \bar{u}}{\partial y}+\bar{v}\frac{\partial u'}{\partial y}\right]=-\frac{\partial p'}{\partial x}-\frac{\mu}{K}u' -2\rho\bar{u}u'+\frac{\mu}{\varepsilon}\left(\frac{\partial^2 u'}{\partial x^2}+\frac{\partial^2 u'}{\partial y^2}+\frac{\partial^2 u'}{\partial z^2}\right) \tag{18}$$

$$\frac{\rho}{\varepsilon^2}\left[u'\frac{\partial \bar{v}}{\partial x}+\bar{u}\frac{\partial v'}{\partial x}+v'\frac{\partial \bar{v}}{\partial y}+\bar{v}\frac{\partial v'}{\partial y}\right]=-\frac{\partial p'}{\partial y}-\frac{\mu}{K}v' -2\rho\bar{v}v'+\frac{\mu}{\varepsilon}\left(\frac{\partial^2 v'}{\partial x^2}+\frac{\partial^2 v'}{\partial y^2}+\frac{\partial^2 v'}{\partial z^2}\right) \tag{19}$$

$$\frac{\rho}{\varepsilon^2}\left[\bar{u}\frac{\partial w'}{\partial x}+\bar{v}\frac{\partial w'}{\partial y}\right]=-\frac{\partial p'}{\partial z}-\frac{\mu}{K}w' +\frac{\mu}{\varepsilon}\left[\frac{\partial^2 w'}{\partial x^2}+\frac{\partial^2 w'}{\partial y^2}+\frac{\partial^2 w'}{\partial z^2}\right] \tag{20}$$

$$\bar{u}\frac{\partial T'}{\partial x}+\bar{v}\frac{\partial T'}{\partial y}+u'\frac{\partial \bar{T}}{\partial x}+v'\frac{\partial \bar{T}}{\partial y} =\alpha\left(\frac{\partial^2 T'}{\partial y^2}+\frac{\partial^2 T'}{\partial y^2}+\frac{\partial^2 T'}{\partial z^2}\right). \tag{21}$$

Following the method of order-of-magnitude analysis prescribed in detail by Hsu and Cheng [2], the terms $\partial u'/\partial x$, $\partial^2 u'/\partial x^2$, $\partial^2 v'/\partial x^2$, $\partial^2 w'/\partial x^2$ and $\partial^2 T'/\partial x^2$ in equations (17)–(21) can be neglected. The omission of $\partial u'/\partial x$ in equation (17) implies the existence of a disturbance stream function ψ' such that

$$w'=\frac{\partial \psi'}{\partial y},\quad v'=-\frac{\partial \psi'}{\partial z}. \tag{22}$$

We assume that the three-dimensional disturbances are of the form

$$(\psi', u', T')=[\tilde{\psi}(x,y), \tilde{u}(x,y), \tilde{T}(x,y)] \times \exp(\mathrm{i}az+\gamma(x)) \tag{23}$$

where a is the spanwise periodic wave number, and

$$\gamma(x)=\int \alpha_i(x)\,\mathrm{d}x$$

with $\alpha_i(x)$ denoting the spatial growth factor. For the lowest order approximation $\gamma(x)=\alpha_i\cdot x$ [2]. It is noted that the amplitudes of the disturbance are assumed functions of both x and y, in contrast to the parallel or quasi-parallel flow model wherein the amplitudes of the disturbance are functions of y only. Setting $\alpha_i=0$ for neutral stability yields

$$\frac{1}{\varepsilon^2}\left[\mathrm{i}a\tilde{u}\frac{\partial \bar{u}}{\partial x}+\mathrm{i}a\bar{u}\frac{\partial \tilde{u}}{\partial x}+a^2\tilde{\psi}\frac{\partial \bar{u}}{\partial y}+\mathrm{i}a\bar{v}\frac{\partial \tilde{u}}{\partial y}-\frac{\partial \bar{u}}{\partial x}\frac{\partial^2\tilde{\psi}}{\partial x\,\partial y} -\bar{u}\frac{\partial^3\tilde{\psi}}{\partial x^2\,\partial y}-\frac{\partial \bar{v}}{\partial x}\frac{\partial^2\tilde{\psi}}{\partial y^2}-\bar{v}\frac{\partial^3\tilde{\psi}}{\partial x\,\partial y^2}\right]=-\frac{v}{K}\left[\mathrm{i}a\tilde{u}-\frac{\partial^2\tilde{\psi}}{\partial x\,\partial y}\right] -2\mathrm{i}ac\bar{u}\tilde{u}+\frac{v}{\varepsilon}\left[\mathrm{i}a\frac{\partial^2\tilde{u}}{\partial y^2}-\mathrm{i}a^3\tilde{u}-\frac{\partial^4\tilde{\psi}}{\partial y^3\,\partial x}+a^2\frac{\partial^2\tilde{\psi}}{\partial x\,\partial y}\right] \tag{24}$$

$$\frac{1}{\varepsilon^2}\left[\mathrm{i}a\tilde{u}\frac{\partial \bar{v}}{\partial x}+a^2\bar{u}\frac{\partial\tilde{\psi}}{\partial x}+a^2\frac{\partial \bar{v}}{\partial y}\tilde{\psi}+a^2\bar{v}\frac{\partial\tilde{\psi}}{\partial y}-\frac{\partial \bar{u}}{\partial y}\frac{\partial^2\tilde{\psi}}{\partial x\,\partial y} -\bar{u}\frac{\partial^3\tilde{\psi}}{\partial x\,\partial y^2}-\frac{\partial\bar{u}}{\partial y}\frac{\partial^2\tilde{\psi}}{\partial y^2}-\bar{v}\frac{\partial^3\tilde{\psi}}{\partial y^3}\right]=\mathrm{i}ag\beta\tilde{T} +\frac{v}{K}\left[\frac{\partial^2\tilde{\psi}}{\partial y^2}-a^2\tilde{\psi}\right]-2a^2c\bar{v}\tilde{\psi} -\frac{v}{\varepsilon}\left[a^4\tilde{\psi}-2a^2\frac{\partial^2\tilde{\psi}}{\partial y^2}+\frac{\partial^4\tilde{\psi}}{\partial y^4}\right] \tag{25}$$

$$\alpha\left(\frac{\partial^2\tilde{T}}{\partial y^2}-a^2\tilde{T}\right)=\bar{u}\frac{\partial\tilde{T}}{\partial x}+\bar{v}\frac{\partial\tilde{T}}{\partial y}+\tilde{u}\frac{\partial\bar{T}}{\partial x}-\mathrm{i}a\tilde{\psi}\frac{\partial\bar{T}}{\partial y}. \tag{26}$$

Equations (24)–(26) are solved based on the local similarity approximations [2], wherein the disturbances are assumed to have weak dependence in the streamwise direction (i.e. $\partial/\partial\xi \ll \partial/\partial\eta$). Letting

$$k=\frac{ax}{G^{1/5}},\quad Q=\frac{\tilde{u}x}{vG^{2/5}},\quad F=\frac{\tilde{\psi}}{5\mathrm{i}vG^{1/5}},\quad \Theta=\frac{\tilde{T}}{(T_w-T_\infty)} \tag{27}$$

we obtain the following system of equations for the local similarity approximations:

$$\frac{1}{\varepsilon}Q''-\left(\frac{1}{\varepsilon}k^2+\xi+2\xi^{5/(4-2m)}Fr^{1/(2-m)}B_3\right)Q -\frac{1}{\varepsilon^2}\{B_1Q+(2m+1)B_3Q-B_2Q'\} =k^{-1}G^{-1/5}[(4m-3)F'''+(m-2)\eta F''''] +\xi k^{-1}G^{-1/5}[(2m+1)F'+(m-2)\eta F''] +kG^{-1/5}[(2m-1)F'+(m-2)\eta F''] +\frac{1}{\varepsilon^2}\{25kG^{-1/5}B_4F-k^{-1}G^{-1/5}B_1[(2m+1)F' +(m-2)\eta F'']+k^{-1}G^{-1/5}(m-2)B_3[(4m+2)F' +(5m-5)\eta F''+(m-2)\eta^2F'''] +k^{-1}G^{-1/5}(m-2)B_5F''+k^{-1}G^{-1/5}B_7[(3m-1)F'' +(m-2)\eta F''']\} \tag{28}$$

$$\frac{1}{\varepsilon}[F''''-2k^2F''+k^4F]+\frac{1}{\varepsilon^2}\{(m+3)B_3k^2F-B_1k^2F$$
$$-B_2k^2F'-(2m+1)B_4F'-(3m-1)B_3F''+B_6F''$$
$$+B_2F'''\}-\frac{2}{5}k^2\xi^{5/(4-2m)}Fr^{1/(2-m)}G^{-1/5}B_7F$$
$$-\xi F''+k^2\xi F=kG^{1/5}\Theta+\frac{1}{\varepsilon^2}\frac{(m-2)}{25}kG^{-1/5}B_5Q \tag{29}$$

$$\Theta''-k^2\Theta-5m\,Pr\,B_3\Theta+B_2\,Pr\,\Theta'$$
$$=B_8\,Pr\,Q+5Pr\,kG^{1/5}B_9F \tag{30}$$

with the boundary conditions

$$F(0)=F'(0)=Q(0)=\Theta(0)=0$$
$$F(\infty)=F'(\infty)=Q(\infty)=\Theta(\infty)=0 \tag{31}$$

where primes indicate derivatives with respect to η. Equation (31) arises from the fact that the disturbances vanish at the wall and in the free stream in the porous medium. The coefficients $B_1(\eta)$–$B_9(\eta)$ in the equations can be expressed as

$$B_1=(2m+1)f'+(4-2m)\xi\frac{\partial f'}{\partial\xi}+(m-2)\eta f''$$
$$B_2=(m+3)f+(4-2m)\xi\frac{\partial f}{\partial\xi}$$
$$B_3=f'$$
$$B_4=f''$$
$$B_5=(m+3)f-10\xi\frac{\partial f}{\partial\xi}+(3m-1)\eta f'+4(m-2)\xi^2\frac{\partial^2 f}{\partial\xi^2}$$
$$-4(m-2)\eta\xi\frac{\partial f'}{\partial\xi}+(m-2)\eta^2f''$$
$$B_6=(2m+1)f'+(4-2m)\xi\frac{\partial f'}{\partial\xi}$$
$$B_7=(m+3)f+(4-2m)\xi\frac{\partial f}{\partial\xi}+(m-2)\eta f'$$
$$B_8=m\theta+\frac{(4-2m)}{5}\xi\frac{\partial\theta}{\partial\xi}+\frac{(m-2)}{5}\eta\theta'$$
$$B_9=\theta'. \tag{32}$$

Equations (29)–(31) constitute a fourth-order system of linear ordinary differential equations for the disturbance amplitude distributions $Q(\eta)$, $F(\eta)$ and $\Theta(\eta)$. For fixed Pr, ε, m, Fr and ξ the solutions Q, F and Θ are eigenfunctions for the eigenvalues G and k.

3. NUMERICAL METHOD OF SOLUTION

The system of equations (11)–(13) was solved by an efficient and accurate implicit finite-difference method similar to that described in Cebeci and Bradshaw [20]. The details are omitted here. In the stability calculations, the disturbance equations are solved by separately integrating four linearly independent integrals. The full equations may be written as the sum of four linearly independent solutions

$$Q=Q_1+D_2Q_2+D_3Q_3+D_4Q_4$$
$$F=F_1+D_2F_2+D_3F_3+D_4F_4$$
$$\Theta=\Theta_1+D_2\Theta_2+D_3\Theta_3+D_4\Theta_4. \tag{33}$$

Four independent integrals (Q_i, F_i, Θ_i), with $i = 1$–4 may be chosen so that their asymptotic solutions are

$$Q_1=0, \quad F_1=E_1e^{H_1\eta}, \quad \Theta_1=e^{H_1\eta}$$
$$Q_2=e^{H_2\eta}, \quad F_2=E_2e^{H_2\eta}, \quad \Theta_2=0$$
$$Q_3=0, \quad F_3=e^{-k\eta}, \quad \Theta_3=0$$
$$Q_4=0, \quad F_4=e^{H_2\eta}, \quad \Theta_4=0 \tag{34}$$

where

$$H_1=\frac{-B_2\,Pr-\sqrt{((B_2\,Pr)^2+4k^2)}}{2}$$
$$H_2=\frac{-B_2/\varepsilon-\sqrt{((B_2/\varepsilon)^2+4(\xi\varepsilon+k^2))}}{2}$$
$$E_1=\varepsilon kG^{1/5}\Big/\Big[H_1^4+\frac{B_2}{\varepsilon}H_1^3-(2k^2+\varepsilon\xi)H_1^2$$
$$-\frac{B_2}{\varepsilon}k^2H_1+(\xi\varepsilon k^2+k^4)\Big]$$
$$E_2=\frac{\frac{(m-2)}{25\varepsilon}kG^{-1/5}B_5}{4H_2^3-2(2k^2+\varepsilon\xi)H_2+3\frac{B_2}{\varepsilon}H_2^2-\frac{B_2}{\varepsilon}k^2}. \tag{35}$$

Equations (28)–(30) with boundary conditions, equations (31), are then solved as follows. For specified Pr, ε, m, Fr, ξ and k, G is guessed. Using equations (34) as starting values, the four integrals are integrated separately from the outer edge of the boundary layer to the wall using the sixth-order Runge–Kutta variable size integrating routine incorporated with the Gram–Schmidt orthogonalization procedure [21] to maintain the linear independence of the four eigenfunctions. The required input of the base flow to the disturbance equations is calculated, as necessary, by linear interpolation of the stored base flow. From the values of the integrals at the wall, D_2, D_3 and D_4 are determined using the boundary conditions $Q(0) = F(0) = \Theta(0) = 0$. The fourth boundary condition $F'(0) = 0$ is satisfied only for the appropriate value of the eigenvalue G. A Taylor series expansion of the fourth condition provides a correction scheme for the initial guess of G. Iterations continue until the fourth boundary condition is sufficiently close to zero (typically $<10^{-7}$).

4. RESULTS AND DISCUSSIONS

In order to generalize, we have formulated the governing equations to permit the calculation of the power law variation of wall temperature. The results presented here are only for the case of an isothermal surface case, i.e. $m = 0$. Moreover, the Prandtl number, Pr, and the porosity, ε, are set equal to 0.72 and 0.98, respectively.

Figure 1 shows the effects of ξ on the dimensionless tangential velocity profile across the boundary layer for $Fr = 20$ and 0. The solid lines denote the results for the case when the inertia, boundary and convective effects are all included ($Fr = 20$). The dashed lines denote the results when the inertia effect is completely neglected ($Fr = 0$), i.e. only the boundary and convective effects are included. It is shown that, as would be expected, the dimensionless tangential velocity decreases with increasing values of ξ; that is, the tangential velocity decreases with decreasing values of K, for a given value of x and ΔT. It is seen that, as the value of ξ is large ($\xi = 20$), the velocity profile looks similar to that obtained from slip boundary assumptions. It is also seen that the inertia effect decreases the maximum tangential velocity and thickens the velocity boundary layer. This is because the form drag of the porous medium is increased when the inertia effect is included. The results also indicate that the inertia effect can be neglected as the value of ξ is small.

The variations of the dimensionless normal component of velocity across the boundary layer are plotted in Fig. 2 for several different values of ξ. It is shown that the dimensionless normal component velocity is positive (i.e. an outflow) near the surface and negative (i.e. an ordinary entrainment effect) in the outer region. In fact, this unusual phenomenon of 'inner region normal velocity component reversal' is common to all buoyancy-induced flows adjacent to horizontal surfaces [22]. It is also seen that as ξ increases, the inner region of the normal velocity component reversal increases. In addition, this reversal region is thicker when the inertia effect is included.

Representative temperature profiles for different values of ξ and for $Fr = 20$ and 0 are shown in Fig. 3. As can be seen from this figure, as ξ increases, the temperature boundary layer thickness increases. Furthermore, the inertia effect tends to thicken the thermal boundary layer.

Numerical solutions of $-\theta'(\xi, 0)$ vs ξ are shown in Fig. 4 for four cases considered, that is, Darcy's model, pure boundary effect, combined boundary and convective effects (i.e. $Fr = 0$, here called two effects) and combined inertia, boundary and convective effects (here called three effects with $Fr = 20$). It is seen that Darcy's solution overpredicts the heat transfer rate and is valid only for large values of ξ. Compared with the solution of the pure boundary effect with that of two effects, it is found that the convective effect is only important if $\xi < 2.5$. Moreover, compared with the two effects with the three effects, it is seen that the inertia effect reduces the heat transfer and its effect is more pronounced when $\xi > 0.6$.

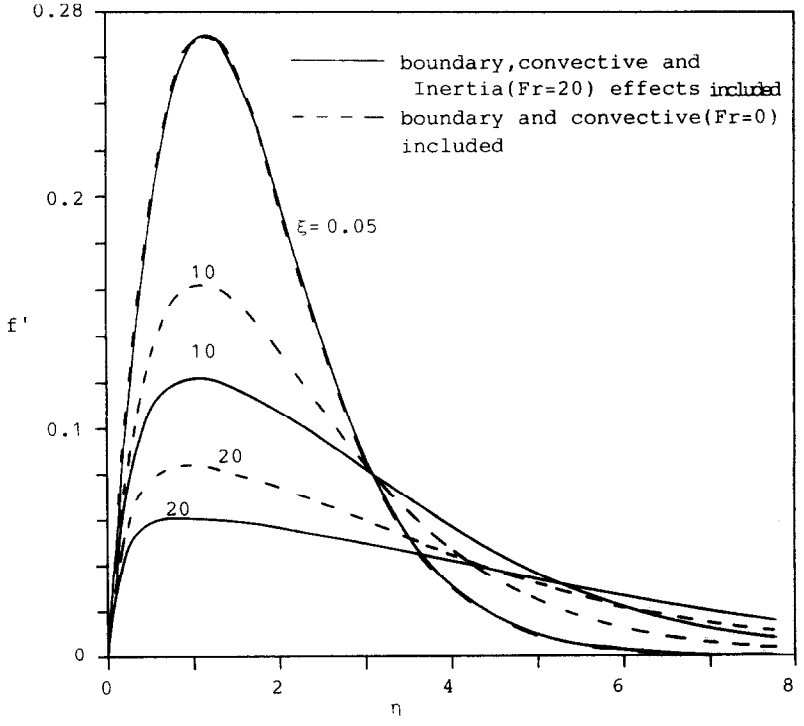

FIG. 1. Dimensionless tangential velocity distribution across the boundary layer as a function of ξ.

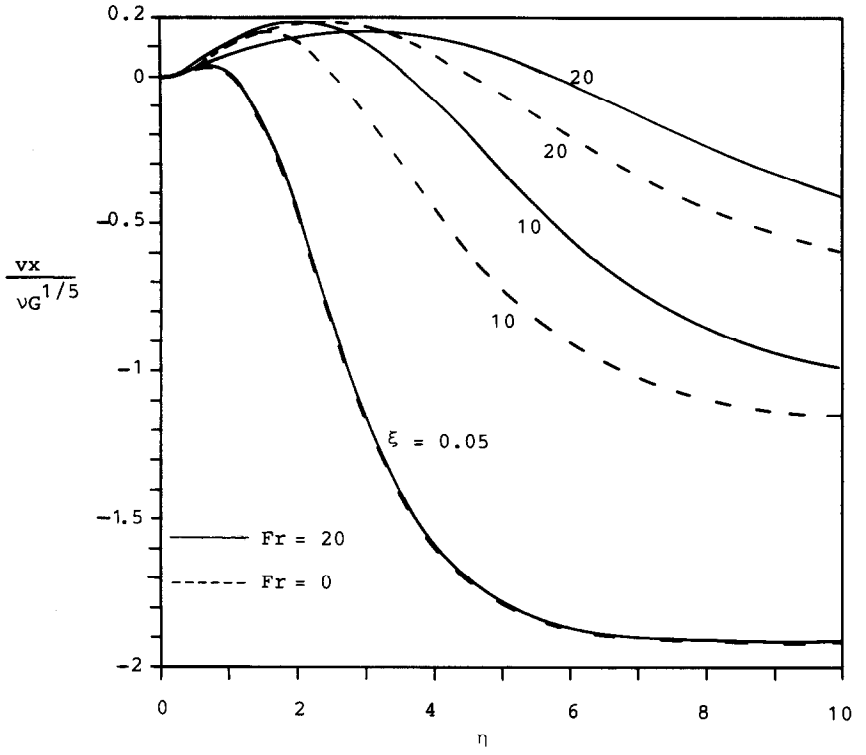

FIG. 2. Dimensionless normal velocity distribution across the boundary layer as a function of ξ.

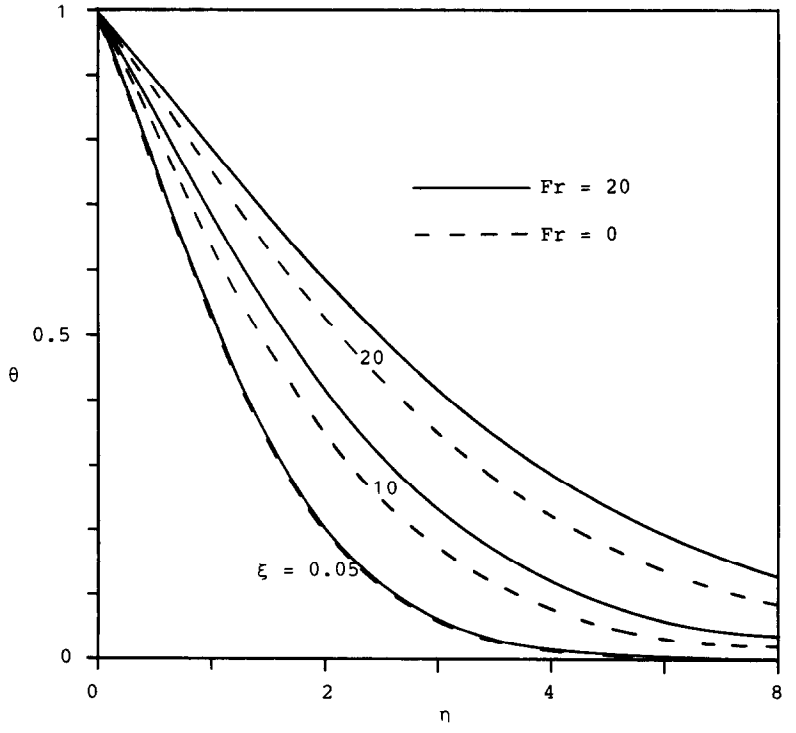

FIG. 3. Dimensionless temperature profile across the boundary layer as a function of ξ.

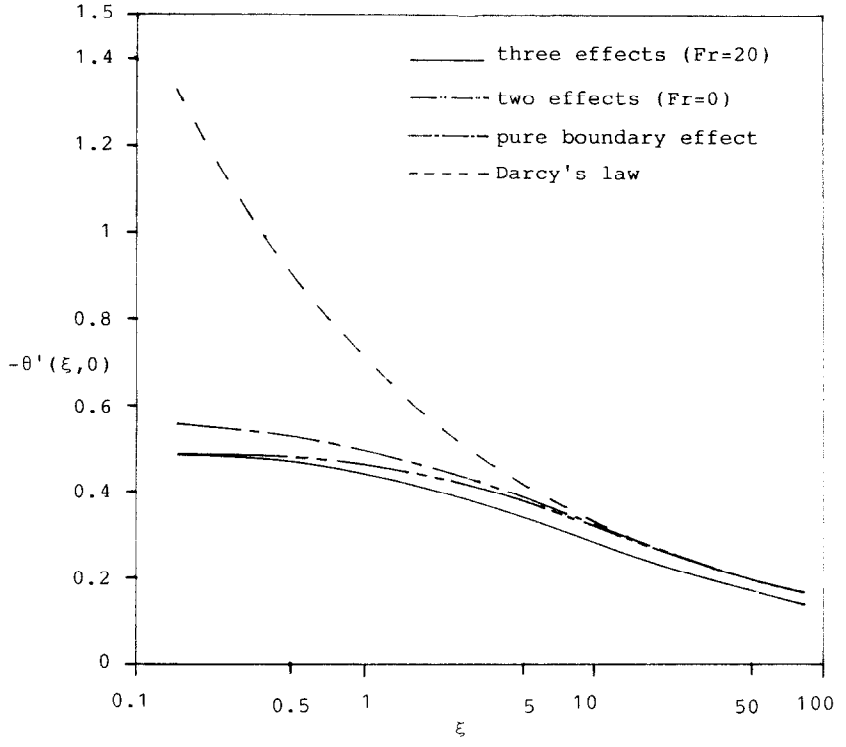

FIG. 4. $-\theta'(\xi,0)$ vs ξ for four cases considered.

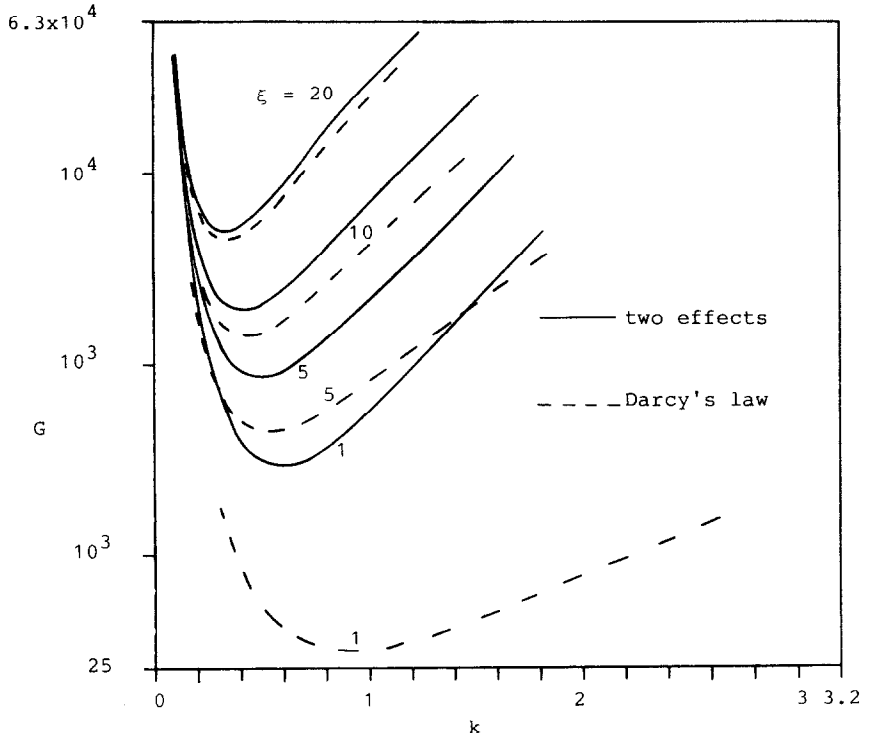

FIG. 5. Comparison of the neutral stability curves between Darcy's model and the two effects for selected values of ξ.

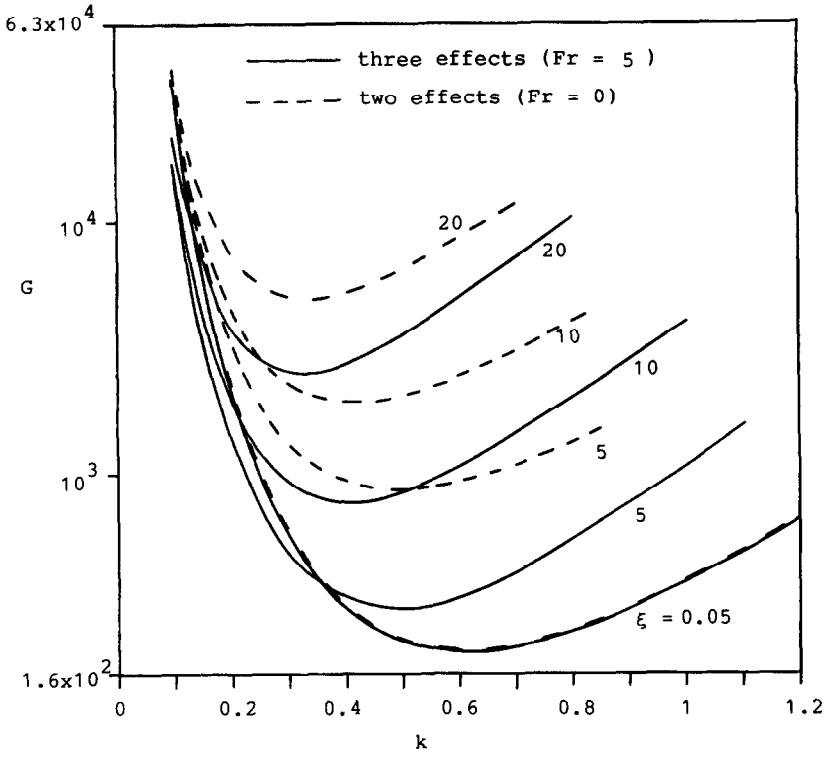

FIG. 6. Comparison of the neutral stability curves between the two effects and the three effects for selected values of ξ.

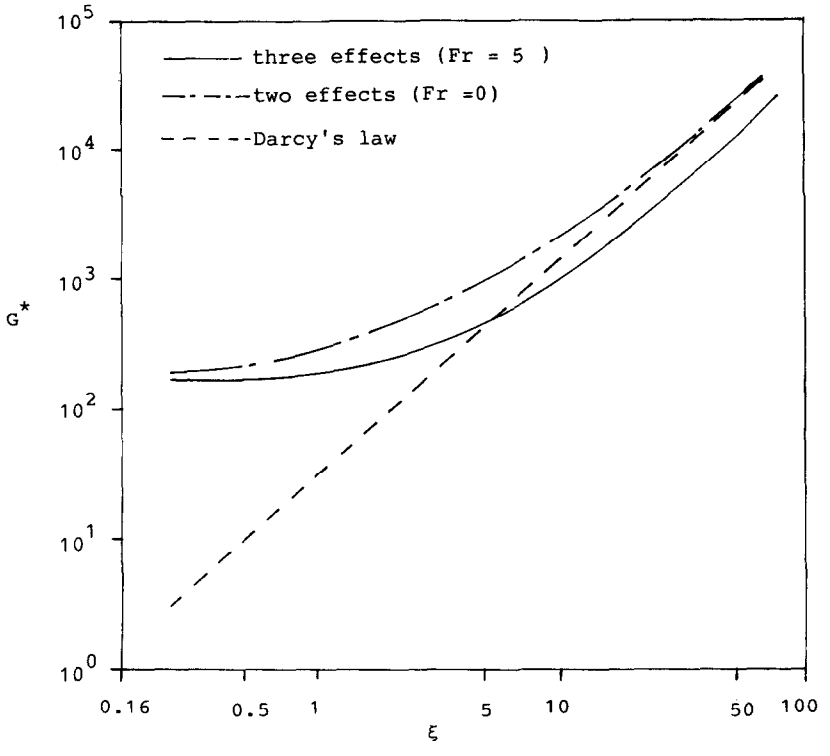

FIG. 7. The critical Grashof number as a function of ξ for Darcy's model, two effects and three effects.

Therefore, it is concluded that, when ξ is small, the discrepancy between the Darcy and non-Darcy model is primarily due to the boundary and convective effects, while as the value of ξ increases, it is primarily due to the inertia effect.

Figure 5 shows the comparison of the neutral stability curves between Darcy's model and the two effects ($Fr = 0$) for selected values of ξ. Note that the case of Darcy's law for a horizontal surface was considered by Hsu *et al.* [1]. To facilitate such a comparison, it is necessary to transform Darcy's model result [1] to (ξ, η) coordinates such that

$$(G)_{ND} = \left[\frac{(Ra_x)_D}{5}\frac{\xi}{Pr}\right]^{5/3}$$

where subscript D denotes Darcy's solutions and ND denotes non-Darcy's solution. It is shown that as ξ decreases, the two sets of neutral stability curves deviate more. On the other hand, for ξ up to 20, these two sets of solutions differ very little. A comparison of the neutral stability curves between the two effects ($Fr = 0$) and the three effects ($Fr = 5$) is plotted in Fig. 6. It can be seen that when the inertia effect is included, the neutral stability curves shift downward, indicating a destabilization of the flow to the vortex instability.

The critical Grashof numbers ($Gr_x/5$), which mark the onset of longitudinal vortices, are plotted as a function of ξ in Fig. 7 for Darcy's model, two effects ($Fr = 0$) and three effects ($Fr = 5$), respectively. When Darcy's model and two effects are compared, it is found that the combined boundary and convective effects stabilize the flow, and these two sets of solutions merge only when ξ is very large ($\xi > 30$). Compared with Darcy's model and the three effects, it is seen that, as $\xi < 6$, the critical Grashof numbers of the three effects are larger than those of Darcy's model, and as ξ decreases the discrepancy increases. However, as $\xi > 6$, the critical Grashof numbers of Darcy's model are larger than those of the three effects. This is because as ξ is small, the stabilizing effect (due to the viscous force and convective term) dominates the destabilizing effect (due to the inertia force). Therefore, the three effects predict the flow is more stable than Darcy's model does. As the value of ξ increases, the destabilizing effect due to the inertia force is more pronounced. Thus the flow predicted by the three effects is less stable than that predicted by Darcy's model.

5. CONCLUSION

The non-Darcian effects on the vortex instability of a horizontal natural convection boundary layer in a saturated high-porosity medium have been examined by a linear stability theory. The numerical results demonstrate that the inertia, boundary and convective effects all reduce the heat transfer rate. The combined boundary and convective effects tend to stabilize the flow and are more pronounced when ξ is small, while the inertia effect tends to destabilize the flow and becomes more significant as the value of ξ is increased.

REFERENCES

1. C. T. Hsu, P. Cheng and G. M. Homsy, Instability of free convection flow over a horizontal impermeable surface in a porous medium, *Int. J. Heat Mass Transfer* **21**, 1221–1228 (1978).
2. C. T. Hsu and P. Cheng, Vortex instability in buoyancy-induced flow over inclined heated surfaces in porous media, *J. Heat Transfer* **101**, 660–665 (1979).
3. J. Y. Jang and W. J. Chang, Vortex instability of buoyancy-induced boundary layer flow in a saturated porous medium, *Int. J. Heat Mass Transfer* **31**, 759–767 (1988).
4. J. Y. Jang and W. J. Chang, The flow and vortex instability of horizontal neutral convection in a porous medium resulting from combined heat and mass buoyancy effects, *Int. J. Heat Mass Transfer* **31**, 769–777 (1988).
5. J. Y. Jang and W. J. Chang, Vortex instability of inclined buoyant layer in porous media saturated with cold water, *Int. Commun. Heat Mass Transfer* **14**, 405–416 (1987).
6. P. Forchheimer, Wasserbewegung Durch Bodeu, *ForschHft. Ver. Dt. Ing.* **45**, 1782–1788 (1901).
7. O. A. Plumb and I. C. Huenefeld, Non-Darcy natural convection from heated surfaces in saturated porous media, *Int. J. Heat Mass Transfer* **24**, 765–768 (1981).
8. A. Bejan and D. Poulikakos, The non-Darcy regime for vertical boundary layer natural convection in a porous medium, *Int. J. Heat Mass Transfer* **26**, 815–822 (1983).
9. P. Cheng and W. J. Minkowycz, Free convection about a vertical flat plate embedded in a porous medium with application to heat transfer from a dike, *Geophys. Res.* **82**, 2040–2044 (1977).
10. H. C. Brinkman, A calculation of the viscous force exerted by a flowing fluid on a dense swarm of particles, *Appl. Scient. Res.* **1**, 27–34 (1970).
11. B. K. C. Chan, C. M. Ivey and J. M. Barry, Natural convection in enclosed porous media with rectangular boundaries, *J. Heat Transfer* **92**, 21–27 (1970).
12. C. T. Hsu and P. Cheng, The Brinkman model for natural convection about a semi-infinite vertical flat plate in a porous medium, *Int. J. Heat Mass Transfer* **28**, 683–697 (1985).
13. T. W. Tong and E. Subramanian, A boundary-layer analysis for natural convection in vertical porous enclosures—use of the Brinkman–extended Darcy model, *Int. J. Heat Mass Transfer* **28**, 563–571 (1985).
14. P. Vasseur and L. Robilland, The Brinkman model for boundary layer regime in a rectangular cavity with uniform heat flux from the side, *Int. J. Heat Mass Transfer* **30**, 717–727 (1987).
15. Y. Katto and T. Masuaka, Criterion for the onset of convective flow in a fluid in a porous medium, *Int. J. Heat Mass Transfer* **10**, 297–309 (1967).
16. K. Walker and G. M. Homsy, A note on convective instability in Boussinesq fluids and porous media, *Trans. ASME J. Heat Transfer* **99**, 338–339 (1977).
17. K. Vafai and C. L. Tien, Boundary and inertia effects on flow and heat transfer in porous media, *Int. J. Heat Mass Transfer* **24**, 195–203 (1981).
18. G. H. Evans and O. A. Plumb, Natural convection from a vertical isothermal surface embedded in a saturated porous medium, *Proceedings of the AIAA–ASME Thermophysics and Heat Transfer Conference*, Paper No. 78-HT-55 (1978).
19. J. T. Hong, C. L. Tien and M. Kaviany, Non-Darcy effects on vertical-plate natural convection in porous media with high porosities, *Int. J. Heat Mass Transfer* **28**, 2149–2157 (1985).

20. T. Cebeci and P. Bradshaw, *Physical and Computational Aspects of Convective Heat Transfer*, Chap. 13. Springer, New York (1984).
21. A. R. Wazzan, T. T. Okamura and H. M. O. Smith, Stability of laminar boundary layer at separation, *Physics Fluids* **190**, 2540–2545 (1967).
22. D. S. Lin and B. Gebhart, Buoyancy-induced flow adjacent to a horizontal surface submerged in porous medium saturated with cold water, *Int. J. Heat Mass Transfer* **29**, 611–623 (1986).

EFFETS NON-DARCIENS SUR L'INSTABILITE TOURBILLONNAIRE D'UN ECOULEMENT HORIZONTAL DE CONVECTION NATURELLE DANS UN MILIEU POREUX

Résumé—On examine les effets non-darciens, en incluant l'inertie, les effets convectifs et de frontière, sur l'instabilité d'un écoulement horizontal de convection naturelle dans un milieu très poreux. Dans l'écoulement de base, les équations de bilan sont résolues en utilisant une transformation de variables et en employant un schéma implicite aux différences finies développé par Keller. L'analyse de stabilité est fondée sur la théorie linéaire de stabilité et les équations qui en résulte sont résoluent à partir d'approximations de similitude locale. Les résultats montrent que tous les trois effets réduisent le transfert de chaleur. De plus, les effets combinés convectifs et de frontière stabilise l'écoulement vers le mode tourbillonnaire de perturbation, tandis que l'effet d'inertie le stabilise.

NON-DARCY-EFFEKTE AUF DIE WIRBELINSTABILITÄT IN EINER HORIZONTALEN NATÜRLICHEN KONVEKTIONSSTRÖMUNG IN EINEM PORÖSEN MEDIUM

Zusammenfassung—Die Non-Darcy-Effekte, wie z. B. Träghheits-, Rand- und konvektive Effekte, auf die Strömung und Wirbelinstabilität in einer horizontalen natürlichen Konvektionsströmung in einem hochporösen Medium werden untersucht. Für die Hauptströmung werden die Erhaltungsgleichungen mit einem geeigneten Variablen-Transformations-Verfahren und einem impliziten Finite-Differenzen-Verfahren von Keller gelöst. Die Stabilitätsanalyse beruht auf der linearen Stabilitätstheorie, die sich daraus ergebenden Gleichungen werden mit örtlichen Ähnlichkeitsansätzen gelöst. Die Ergebnisse zeigen, daß alle drei genannten Effekte den Wärmeübergangskoeffizienten verringern. Weiterhin stabilisieren die kombinierten Rand- und Konvektions-Effekte die Strömung bezüglich der Wirbelinstabilität, während die Trägheitseffekte einen destabilisierenden Einfluß haben.

ЗАВИСИМОСТЬ ВИХРЕВОЙ НЕУСТОЙЧИВОСТИ ГОРИЗОНТАЛЬНОГО ЕСТЕСТВЕННОКОНВЕКТИВНОГО ТЕЧЕНИЯ В ПОРИСТОЙ СРЕДЕ ОТ ЭФФЕКТОВ, НЕ СВЯЗАННЫХ С ЗАКОНОМ ДАРСИ

Аннотация—Исследуется влияние на течение и вихревую неустойчивость горизонтального естественноконвективного пограничного течения в высокопористой среде таких не связанных с законом Дарси эффектов, как инерционные, граничные и конвективные. Определяющие уравнения для основного течения решаются с помощью соответствующих преобразований переменных и разработанной Келлером неявной конечно-разностной схемы. Анализ устойчивости выполнен в линейном приближении, а полученные уравнения для возмущений решаются на основе локального преобразования подобия. Результаты показывают, что все эти три эффекта снижают интенсивность теплопереноса. Кроме того, смешанные граничные и конвективные эффекты стабилизируют течение относительно вихревых возмущений, в то время как инерционный эффект вызывает его дестабилизацию.